ISBN: 978-3-95450-204-2 ISSN: 2673-5350 doi:10.18429/JACoW-IBIC2019-TUPP042

TURN-BY-TURN SYNCHROTRON RADIATION TRANSVERSE PROFILE MONITOR FOR IOTA*

N. Kuklev†, Y.-K. Kim, University of Chicago, Chicago, IL 60637, USA

Abstract

The Integrable Optics Test Accelerator is a research electron and proton storage ring recently commissioned at Fermilab. A key part of its beam diagnostics suite are synchrotron radiation monitors, used for measuring transverse beam profile, position, and intensity. So far, this system has used only visible light cameras, which are optimal for orbit measurements but do not provide turn-by-turn temporal resolution needed for beam dynamics analysis. Current electrostatic BPM system, while capable of turn-by-turn acquisition, will be pushed to its limits of accuracy and linearity by the requirements of planned nonlinear integrable optics experiments, and furthermore does not provide transverse profile data. To address these drawbacks, we present in this paper the design of a turn-by-turn BPM system based on a multi-anode photomultiplier detector. Extensive simulations are shown, combining both particle and optics tracking. A potential hardware and readout architecture is described. Statistical and systematic errors are explored. We conclude by outlining the prototype testing plans for run 2 in the fall of 2019, and other future work.

INTRODUCTION

The Integrable Optics Test Accelerator is a research electron and proton storage ring recently commissioned at Fermilab. It has a circumference of 40m, and is designed to use either 2.5 MeV protons provided by an RFQ injector, or up to 150 MeV electrons from FAST linac [1]. Over next few years, a comprehensive experimental campaign is planned including tests of techniques for improving beam intensity and stability (with integrable optics [2–4], and electron lenses [5]), a demonstration of optical stochastic cooling [6], single electron quantum optics and undulator radiation studies [7].

A wide variety of supporting instrumentation is installed in IOTA, with most capable of quick customization to suit specific experimental needs. One such system are synchrotron radiation monitors, used as transverse profile monitor (TPMs), for measuring transverse beam profile, position, and intensity. So far, this system has used visible light cameras, which are optimal for orbit measurements [8] but do not provide turn-by-turn temporal resolution due to CMOS technology and signal-to-noise limitations. However, such data is of interest for beam dynamics experiments, since the electrostatic BPMs (that provide TBT positions) have a high minimum current limit at which there exists significant intra-beam scattering, preventing true 'few-particle, pencil beam' dynamics observations. Low current beam position data can improve and shorten measurements of dynamic aperture size/tune shifts, and in the ultimate limit of a single electron, would yield true single-particle dynamics. In this paper, we propose a TBT TPM system based on a multi-anode photomultiplier. In the following sections, detailed simulation and a potential hardware design are presented, along with some experimental plans for run 2.

Background and SR System Overview

Synchrotron radiation is produced by charged particles undergoing radial acceleration, and is a byproduct in any storage ring. It plays a large role in beam damping, and is also a commonly used diagnostic signal [9, 10]. SR intensity profile is strongly forward peaked, with total radiation power scaling as fourth power of particle energy. For IOTA, protons do not produce sufficiently intense or energetic SR signal, but for electrons, critical wavelength is in the UV range, allowing for simple and cost effective measurements with visible band optics.

IOTA ring contains 8 bending dipole magnets, with 4 each of 30 and 60 degree varieties, as shown in Fig. 1. All the vacuum chambers have downstream optically transparent windows, through which SR can be extracted. In 4 of 8 sections, radiation from potential insertion devices in the straights can also be observed.

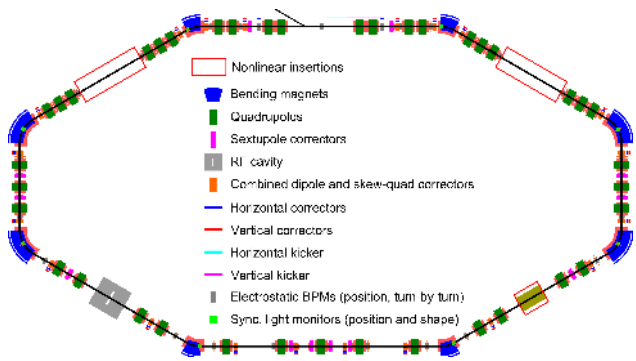

Figure 1: Layout of IOTA ring, with injection point in the upper central section. Main bends are in blue.

SyncLight system is comprised of 8 stations situated atop each of the dipoles. In base configuration, each station has two components - first is an optical periscope transport line consisting of two mirrors, an iris, and a lens, that captures SR and focuses it onto the detector, while using the iris to limit depth of field errors. Second and more extensive part is the modular detector station, that in its base configuration contains a low-noise CMOS camera, but also provides capability to add modules like color wheels, photomultipliers

* This work was supported by the U.S. National Science Foundation under award PHY-1549132, the Center for Bright Beams. Fermi Research Alliance, LLC operates Fermilab under Contract DE-AC02-07CH11359 with the US Department of Energy.
† nkuklev@uchicago.edu

ISBN: 978-3-95450-204-2 ISSN: 2673-5350 doi:10.18429/JACoW-IBIC2019-TUPP042

(PMTs), polarizers, and other devices. It houses various connectivity and support electronics, including Raspberry Pi motor control nodes and fanouts for add-on connectivity - power, Ethernet, shielded high voltage and heliax signal cables. All key components are motorized, allowing for remote alignment and changes to the optical configuration. A typical station is shown in Fig. 2.

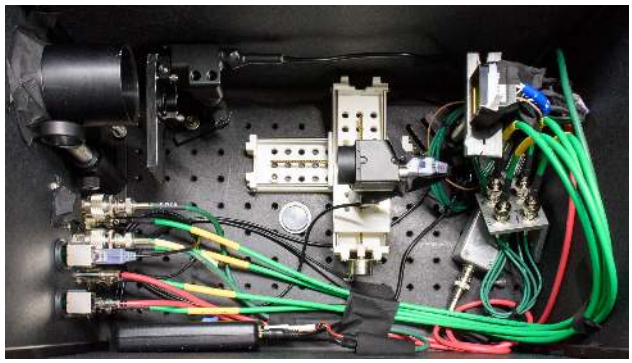

Figure 2: SL station with PMT addon module installed. Image courtesy of G. Stancari.

TURN-BY-TURN PMT SYSTEM

Proposed design of the TBT module follows general SR system philosophy in that it is modular and compatible with existing hardware architecture. However, this does not constrain the design significantly, since there is flexibility to swap optical elements as needed. We assume that all required infrastructure will be available, and that hardware will perform within specifications. The discussion below focuses instead on various design choices, with quantitative analysis wherever possible. Note that the choice of PMT as the base device was dictated by availability of specific M64 tubes and the well-understood PMT properties in very low intensity conditions. The other candidate technology, multi-pixel photon counters based on SiPM (avalanche diode) arrays, are a promising alternative, especially at single-electron current levels, and might be tested in future iterations.

SR Station Selection

Experimental requirements are the main factor in setting the lattice configuration. For nonlinear integrable optics and single electron studies, the primary potential users of TBT capability, in the former case lattice must satisfy a number of strong constraints which effectively fix optical functions, leaving little room for adjustment. Considering mirror symmetry of IOTA, this leaves 4 possible lattice parameter sets to choose from (up to slight differences from opposite sides of magnets being sampled in mirror pairs). Furthermore, 60 degree dipoles have a different set of systematics due to light pickup point being in the arc midpoint, while 30 degree setups see edge radiation. IOTA lattice, with lines denoting SR sampling points, is shown in Fig. 3.

To keep system cost low, we assume use of off-the-shelf symmetric optics (i.e. no special lens shapes or coatings).

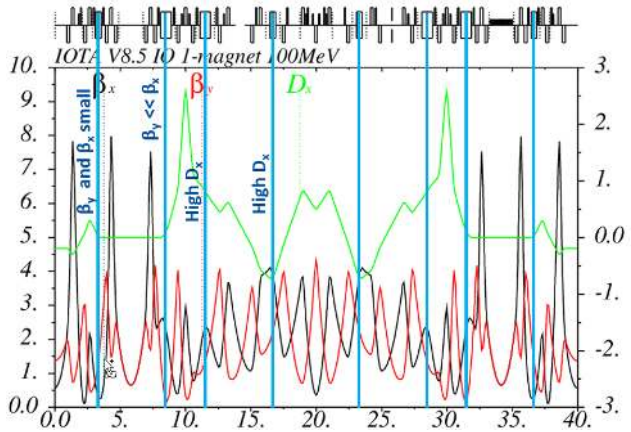

Figure 3: IOTA lattice for nonlinear integrable optics experiments. Blue lines denote candidate SR sampling locations.

This implies that in order to optimize detector area utilization, a location with near equal β_x/β_y is desired such that H/V oscillation amplitudes are the same (planes will mix due to coupling, even if initially unequal). For most measurements, it is also preferable to have low dispersion, which might otherwise complicate data analysis due to power supply noise as well as path lengthening (and hence energy and position changes). Optical magnification can be tuned for desired aperture and resolution tradeoff as the final step, regardless of actual β values, since beam size is significantly above diffraction limits.

Given above considerations, M1R (upper right 30 degree magnet) was chosen as the default position. It has small dispersion at the entrance, and betas are within a factor of 2 and sufficiently small to avoid any window aperture issues. Note that M1L is another candidate, trading ~2x more β-function disparity for completely zeroed out dispersion.

Beam Dynamics Simulations

To establish SR source parameters, we performed 6D symplectic tracking using code 'elegant'. A representative distribution, similar to those observed in run 1 nonlinear optics studies, was tracked in a full IOTA lattice at 150MeV with several misalignment seeds to establish equilibrium distribution. Then, a single-turn combined horizontal and vertical kick at half the maximum aperture was applied, simulating a typical tune shift measurement, and beam parameters at point of SR emission recorded. Representative X-Y projections of such a simulation are shown in Fig. 4.

Optics Simulation

Beam parameters were imported into the Synchrotron Radiation Workshop (SRW), with python library wrapper being used for subsequent analysis. Optical setup followed that of the CMOS camera, with only a single focusing lens and distances set to achieve a zoom level so as to fit ±1.4 mm aperture within 18 mm PMT window. SR wavefronts were generated in bending magnet, propagated to the image plane (ignoring mirrors for simplicity), and downsampled as if

ISBN: 978-3-95450-204-2 ISSN: 2673-5350 doi:10.18429/JACoW-IBIC2019-TUPP042

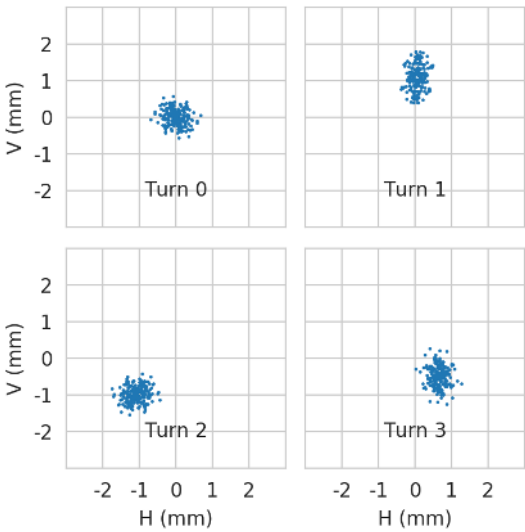

Figure 4: XY projections of four successive turns of a 200 particle bunch, with kick being applied after turn 0.

measured by the PMT. Random noise of 2% was then added, as well as 1% nearest-neighbor cross-talk. Initial and down-sampled images for a typical run are shown in Fig. 5.

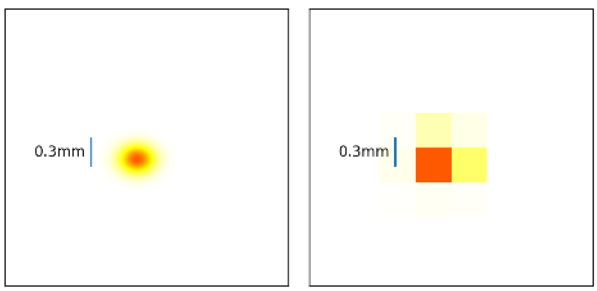

Figure 5: Simulated ideal and PMT-sampled images.

Signal Simulation

Producing simulated pulse signals, and converting them back into intensities, as would be done with real signals, was not simulated since such process must be tailored to specific PMT and DAQ characteristics. Instead, using above simulated PMT pixel intensities directly, beam position reconstruction was performed by fitting a 2D Gaussian function with free rotation parameter. Using Gaussian assumption on beam shape is reasonable since previous experimental results showed good fit quality in most lattice configurations, especially after median noise filtering and background subtraction. Distribution moments were used as initial guesses, which improved convergence. Moments could also be used as a first estimate during online processing.

A test set of 200 simulated beam parameter seeds was generated and fitted, with accuracy metric of mean absolute error in x and y centroid positions. Resulting distribution is shown in Fig. 6. Note how accuracy drops going outwards due to increasing image distortions and in extreme cases distribution edges falling past the edge of the detector. However, even with worst case errors the signal quality is comparable to that of run 1 BPMs, suggesting that tunes should be obtainable at required precision with 50-100 turns using NAFF procedure. Detailed simulations are ongoing.

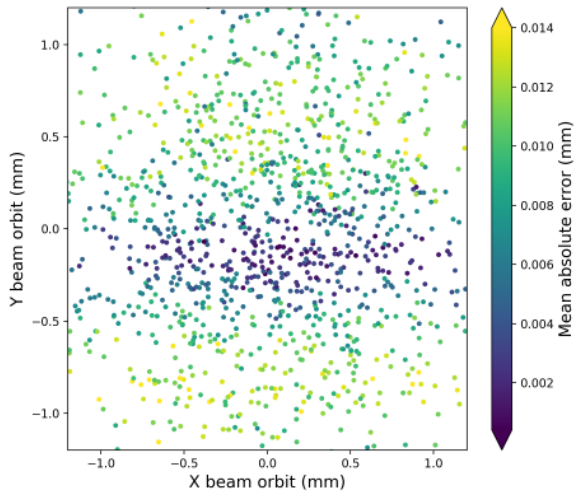

Figure 6: Mean position error from random simulated PMT data analysis. Error bars too small to show, ~ $5x10^{-4}$.

Unfortunately, with only an 8x8 detector, reconstruction of sigma matrix is impractical in the large aperture configuration. However, for observations near closed orbit (i.e. when beam image size ~ detector size), that is not the case. Such a setup can be relevant for few/single electron studies, and detailed intensity simulations are ongoing to predict the noise floor and required minimum number of particles.

EXPERIMENTAL IMPLEMENTATION

PMT

For the prototype station, it is proposed to use an already available Hamamatsu M64 PMT from one of spare MINOS modules [11], shown in Fig. 7, since it provides sufficient QE and low dark current. The appropriate base is also available. In an ideal case, final design would employ a 256-channel modern MCP design, which would enable better signal timing while increasing resolution and/or aperture.

Figure 7: Hamamatsu R5900-00-M64 with base adapter.

ISBN: 978-3-95450-204-2 ISSN: 2673-5350 doi:10.18429/JACoW-IBIC2019-TUPP042

DAQ

For IOTA bunch length (10 cm), revolution period (133 ns) and typical pulse FWHM (5-10 ns, <1 ns rise time) (see Figs. 8 and 9), there is little room to multiplex signals, but acquiring a commercial 64 channel simultaneous ADC of required speed and bandwidth (2GS/s, 1GHz) is expensive. There are promising pilot projects with ring-resonator ADCs which have planned cost of <$100/ch, and ~$500/ch is currently available from major vendors like Teledyne for bulk orders. An alternative approach is to use integrator circuits with gating around the revolution marker, which would trade off pulse information for significantly slower readout requirements. For initial proof of concept, we plan to use 2 x 4ch scopes, providing 8 quadrants, and opportunistically test various devices for the full DAQ system.

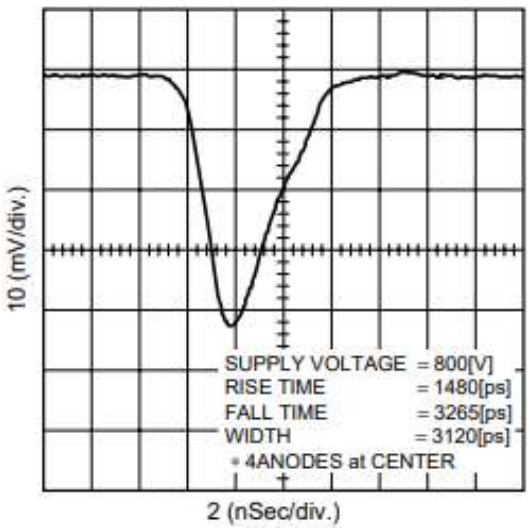

Figure 8: Expected M64 pulse shape.

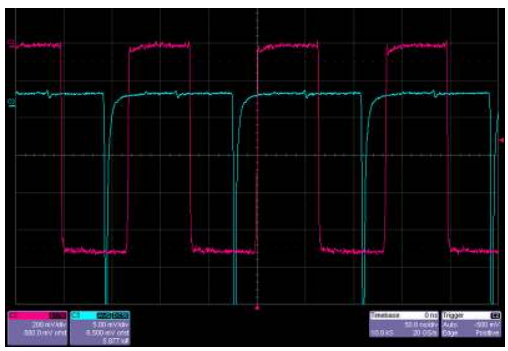

Figure 9: Test MCP-PMT measurement during run 1. Square wave represents revolution marker.

CONCLUSION

We have presented the design and simulated performance of a proposed TPM extension to the IOTA SR system. High fidelity simulations were performed, taking into account experimental lattice parameters and misalignments, to generate and propagate SR onto the multi-anode PMT detector. Based on accuracy of recovered beam positions under nominal noise conditions, we have determined that even an 8x8 detector is capable of providing sufficient position resolution for tune determination. For run 2 starting in the fall of 2019, we plan to perform a trial run using only 8 channels to validate the setup and test sensitivity limits, while continuing to explore economical full array readout options.

ACKNOWLEDGEMENTS

The authors wish to thank A. Romanov and G. Stancari for supervision, discussions, and experimental help.

REFERENCES

[1] S. Antipov *et al.,* "IOTA (Integrable Optics Test Accelerator): facility and experimental beam physics program," *J. Instrum.*, vol. 12, no. 03, pp. T03002, Mar. 2017. doi:10.1088/1748-0221/12/03/T03002

[2] V. Danilov and S. Nagaitsev, "Nonlinear accelerator lattices with one and two analytic invariants," *Phys. Rev. ST Accel. Beams*, vol. 13, p. 084002, Mar. 2010. doi:10.1103/PhysRevSTAB.13.084002

[3] S.A. Antipov, S. Nagaitsev, and A. Valishev. "Single-particle dynamics in a nonlinear accelerator lattice: attaining a large tune spread with octupoles in IOTA," *J. Instrum.*, vol. 12, no. 04, Apr. 2017. doi:10.1088/1748-0221/12/04/P04008

[4] N. Kuklev, Y. K. Kim, S. Nagaitsev, A. L. Romanov, and A. Valishev, "Experimental Demonstration of the Henon-Heiles Quasi-Integrable System at IOTA", in *Proc. IPAC'19*, Melbourne, Australia, May 2019, pp. 386–389. doi:10.18429/JACoW-IPAC2019-MOPGW113

[5] Y. S. Derbenev, "Theory of electron cooling," Jun 2017, arXiv:1703.09735

[6] V. Lebedev, "Optical Stochastic Cooling," *ICFA Beam Dyn. Newslett.*, vol. 65, pp. 100–116, 2014. https://icfa-usa.jlab.org/archive/newsletter/icfa_bd_nl_65.pdf

[7] I. Lobach *et al.*, "Study of Fluctuations in Undulator Radiation in the IOTA Ring at Fermilab,"in *Proc. IPAC'19*, Melbourne, Australia, May 2019, pp. 777–780. doi:10.18429/JACoW-IPAC2019-MOPRB088

[8] N. Kuklev, J. D. Jarvis, Y. K. Kim, A. L. Romanov, J. K. Santucci, and G. Stancari, "Synchrotron Radiation Beam Diagnostics at IOTA - Commissioning Performance and Upgrade Efforts,"in *Proc. IPAC'19*, Melbourne, Australia, May 2019, pp. 2732–2735. doi:10.18429/JACoW-IPAC2019-WEPGW103

[9] R. Thurman-Keup *et al.*, "Synchrotron radiation based beam diagnostics at the Fermilab Tevatron," *J. Instrum.*, vol. 6, no. 09, pp. T09003, Sep. 2011. doi:10.1088/1748-0221/6/09/T09003

[10] R. Jung, P. Komorowski, L. Ponce, and D. Tommasini, "The LHC 450-GeV to 7-TeV synchrotron radiation profile monitor using a superconducting undulator," in *Proc. AIP Conf.*, vol. 648, pp. 220–228, 2003, doi:10.1063/1.1524404

[11] M. A. Barker *et al.*, "Testing of Hamamatsu R5900-00-M64 Multi-Pixel PMTs for MINOS," arXiv:hep-ex/0203001